Multicomponent Nanosystem for Low-Dose, Low-Energy X-Ray-Activated Cancer Treatment

Melissa Santi[1,2], Gloria Cenci[3,4], Silvana Pinelli[5], Marco Villani[3], Marco Bormetti[4], Elena Ferrari[3], Valentina Sinisi[3], Pragati More[6], Bengt Fadeel[6], Evie L. Papadopoulou[7], Francesco Bonaccorso[7], Franca Bigi[4], Giancarlo Salviati[3], Rossi Francesca[3]

1) Istituto Nanoscienze (NANO-CNR) e Scuola Normale Superiore, 56127 Pisa, Italy. 2) Istituto di Biofisica (IBF-CNR), 56124 Pisa, Italy (melissa.santi@cnr.it) 3) CNR-IMEM, 43124 Parma, Italy . 4) Department of Chemistry, Life Sciences and Environmental Sustainability, University of Parma, 43124 Parma, Italy. 5) Department of Medicine and Surgery, University of Parma, 43126 Parma, Italy. 6) Institute of Environmental Medicine, Karolinska Institutet, 17177 Stockholm, Sweden. 7) BeDimensional S.p.A., 16163 Genova, Italy.

BACKGROUND

Cancer remains one of the leading causes of mortality worldwide, and conventional treatments such as photodynamic therapy (PDT) and radiotherapy often suffer from limited efficacy and significant side effects.[1] To address these challenges, we developed a biocompatible hybrid nanosystem based on two-dimensional tungsten disulfide (WS_2) nanoflakes, decorated with gold nanoparticles and further functionalized with a porphyrin derivative, an approach that integrates nanomaterials engineering, plasmonic nanotechnology, and photoactive molecular design within a single multifunctional platform. The high atomic number of WS_2 and Au enhances local X-ray absorption, promoting the generation of secondary electrons and reactive oxygen species (ROS), while the porphyrin moiety contributes additional photophysical activity, yielding a radiosensitizer designed to be activated by low-energy, low-dose X-ray irradiation for selective enhancement of cancer cell killing. The nanosystem's physicochemical properties were characterized, and its biological performance was evaluated in vitro using HT-29 human colorectal cancer cells. Cellular internalization and therapeutic response to low-dose irradiation (2 Gy, 40 keV) were assessed through gene expression analysis (SOD1, HMOX1, BAX, and BCL2), cell cycle modulation, apoptosis induction, and clonogenic survival assays. Overall, these findings highlight the potential of this hybrid 2D nanomaterial-based system as an effective, biocompatible radiosensitizer for low-dose radiotherapy applications, opening new avenues for the design of multifunctional nanoplatforms in cancer nanomedicine.[2]

RESULTS

1. Synthesis and characterization of THPP@AuNPs@WS_2 nanosystem

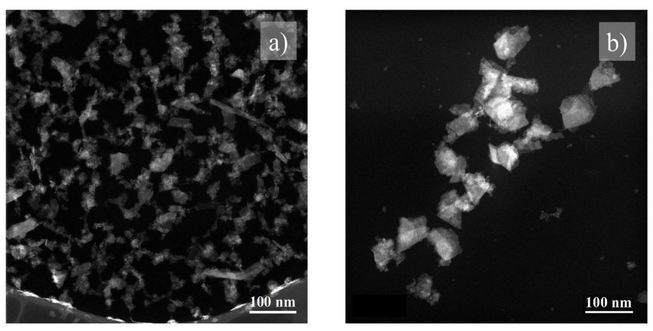

Figure 1: Exfoliated WS_2 flakes. (a,b) STEM-HAADF images of ensembles of WS_2 flakes produced by LPE of WS_2 single crystal in IPA.

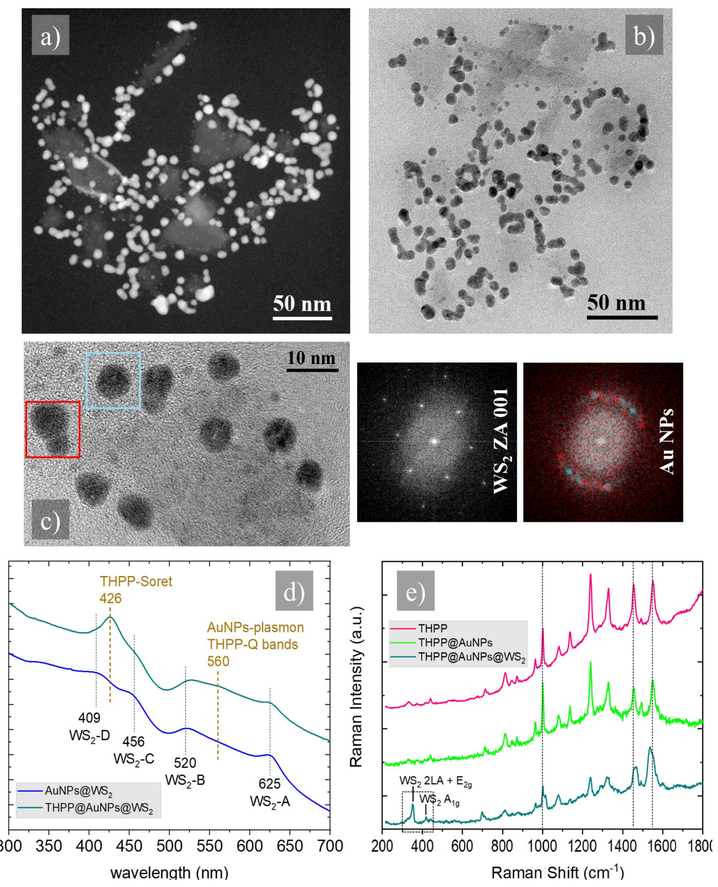

Figure 2: Multicomponent nanosystems. Representative STEM-HAADF image (a) and TEM image (b) of AuNPs@WS_2 flakes. (c) HR-TEM image, with corresponding FFT acquired on the WS_2 lattice (left) and AuNPs (right). (d) UV-Visible absorption spectra of AuNPs@WS_2 and THPP@AuNPs@WS_2 nanosystems. (e) Raman spectra of a THPP 10-3 M water solution (pink curve), a THPP@AuNPs dispersion (green curve), and a THPP@AuNPs@WS_2 dispersion (dark cyan curve). The spectra were acquired with laser excitation at 532 nm. The vertical dashed lines mark the three porphyrin bands at 1001, 1454 and 1549 cm-1 which are broadened in the complete nanosystem.

Au nanoparticles (5–20 nm) were successfully photochemically grafted onto few-layer WS_2 nanoflakes through a surfactant-free and scalable approach, enabling controlled AuNP coverage while preserving the structural integrity and crystallinity of WS_2.[3,4] TEM and HR-TEM analyses confirmed the formation of crystalline AuNPs anchored onto highly crystalline WS_2 nanoflakes. The hybrid platform was subsequently functionalized with a PEGylated, thiol-terminated tetra(4-hydroxyphenyl)porphyrin (THPP) derivative, yielding a stable and water-dispersible photosensitizing nanosystems. UV–Vis and Raman spectroscopy confirmed the successful conjugation of THPP, while TEM and DLS demonstrated that the functionalization did not affect the morphology, size, or dispersion of the nanostructure.

2. Biocompatibility of nanosystems in primary human immune cells

Immune biocompatibility of the THPP@AuNPs@WS_2 nanosystems was further assessed in primary human PBMCs from healthy donors by evaluating cytokine and chemokine secretion after 24 h exposure using a multi-plex array (Fig. 3). While LPS (0.1 µg/mL) induced a robust proinflammatory response, as reflected in the heatmap (Fig. 5a) and confirmed for IL-1β and TNF-α (Fig. 3b, c), the nanosystems did not elicit significant proinflammatory cytokine release. Only IL-13 and MDC (CCL22), two Th2-associated mediators involved in allergic responses, showed a modest but statistically significant increase relative to control (Fig. 3d, e), whereas Na_2WO_4 (25 mM), used as a positive control for tungstate-induced toxicity, had no effect on these markers. These findings confirm that the de novo designed THPP@AuNPs@WS_2 nanosystems are immunologically biocompatible with primary human immune cells from healthy donors.

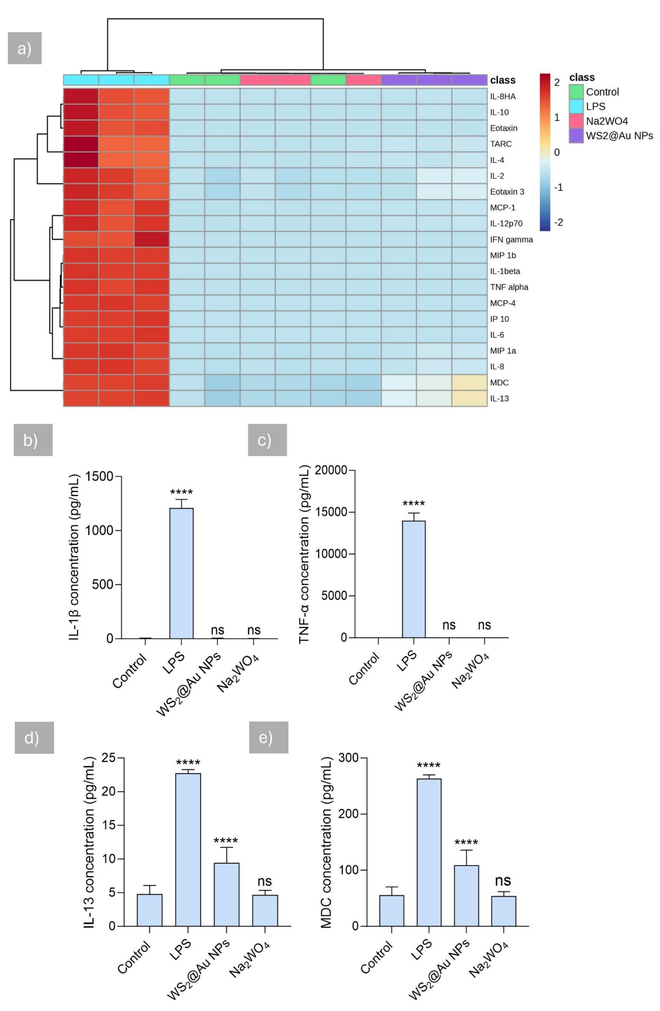

Figure 3: Profiling of cytokine and chemokine secretion. PBMCs isolated from three human donors were exposed for 24 h to THPP@AuNPs@WS_2 or to the soluble salt, Na_2WO_4 (positive control for cell death). LPS was included as a positive control for inflammation. (a) Samples were analyzed using a multi-plex array and hierarchical clustering analysis was conducted to visualize relationships between the various biomarkers and conditions. Shorter branches indicate greater similarity between samples. The dendrograms on the left and top of the heatmap represent the clustering of samples and cytokines/chemokines, respectively. The results are shown for each individual donor to illustrate the concordance between the three donors. (b-e) Expression (secretion) of (b) TNF-α, (c) IL-1β, (d) IL-13, and (e) MDC (macrophage-derived chemokine, also known as CCL22). For clarification, the results shown in the heatmap and those reported in the graphs below are derived from the same experiments. Results in (b-e) are plotted as mean values ± S.D. using cells from three donors. ****p < 0.0001.

3. THPP@AuNPs@WS_2 promote X-ray-triggered cancer cell killing, proliferation arrest and intra-cellular oxidative stress.

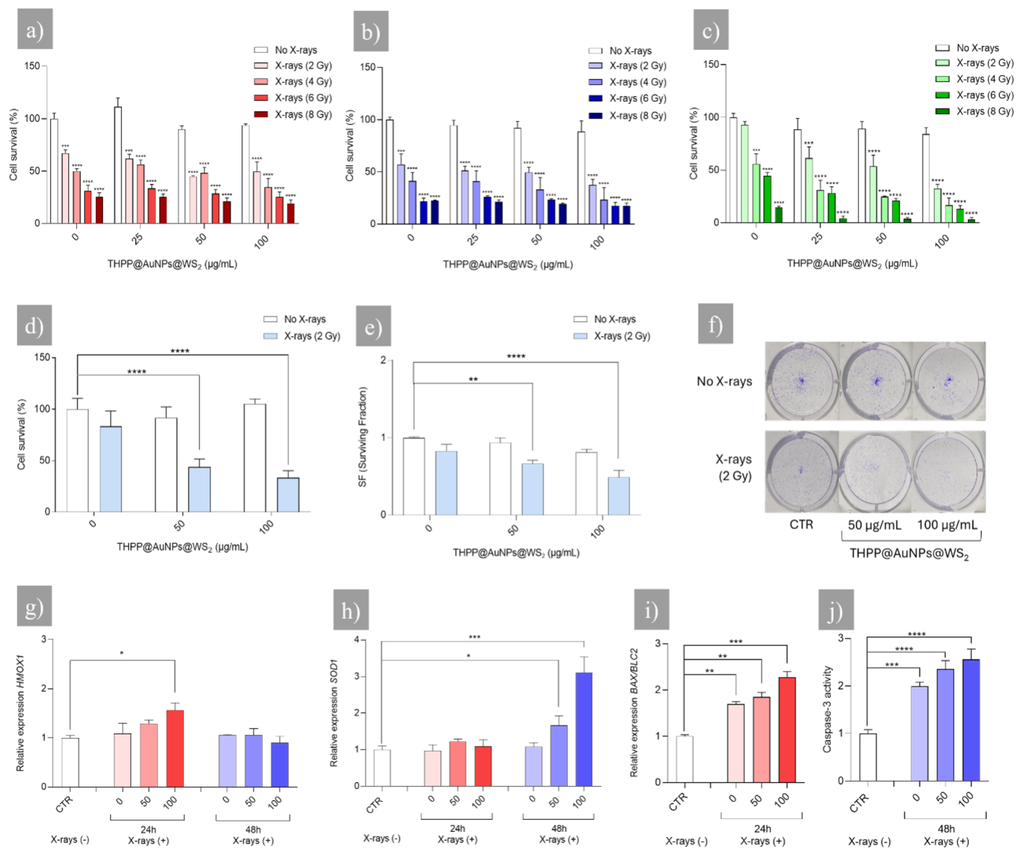

Fig. 4. HT-29 cells were exposed to X-ray irradiation (2, 4, 6 and 8 Gy), in the presence or absence of THPP@AuNPs@WS_2 at the indicated concentrations, and cell survival was determined at 24 h (a), 48 h (b), 72 h (c) and 7 days (d) post X-rays by cell counting. (e) Clonogenic growth was monitored and plotted as surviving fraction "SF" of HT-29 cells exposed to THPP@AuNPs@WS_2 at the indicated concentrations, with or without 2 Gy irradiation. Colonies were counted after 7 days of incubation, and the SF of each cell group was normalized to the plating efficiency (PE) of control cells not exposed to either the nanosystems or X-rays. (f) Representative images of cell colonies. Relative gene expression levels of *HMOX1* (g), *SOD1* (h), and *BAX*/*BCL2* ratio (i) in HT-29 cells treated with 0, 50 or 100 µg/mL of THPP@AuNPs@WS_2 after 24 h and 48 h from 2 Gy X-rays. (j) Effects on caspase-3 activity in HT-29 cells treated with 0, 50 or 100 µg/mL of THPP@AuNPs@WS_2 after 48 h from 2 Gy X-rays. For all the graphs, percentage values were normalized to the untreated control and significance is expressed relative to untreated control for each time point. The results shown are mean values ± S. D (n = 3). *p < 0.05, **p < 0.01, ***p < 0.0002, ****p < 0.0001.

Cellular uptake of the nanosystems was confirmed by TEM, and localized within intracellular endosomal compartments. To assess radiosensitizing potential, cells were exposed to increasing X-ray doses combined with different nanosystem concentrations. THPP@AuNPs@WS_2 induced a dose- and concentration-dependent cytostatic effect, and unlike irradiation alone, prevented cell proliferation recovery over time (Fig. 3a–d). This radiosensitizing activity was confirmed by colony formation assays, showing a significant reduction in surviving fraction only when X-rays were combined with the nanosystem (Fig. 3e, f), and outperformed the bicomponent THPP@AuNPs control. At the molecular level, combined treatment upregulated oxidative stress-related genes (HMOX1, SOD1) and increased the BAX/BCL2 ratio and caspase-3 activity, indicating enhanced ROS production and activation of the intrinsic apoptotic pathway (Fig. 3g–j). Consistently, flow cytometry showed increased G2/M arrest and a higher sub-G0/G1 apoptotic fraction in cells treated with the combination (Fig. 5), together with elevated γH2AX DNA damage foci. Overall, these results indicate that THPP@AuNPs@WS_2 enhances X-ray-induced cytotoxicity in cancer cells through a combined physical dose-enhancement and ROS-mediated apoptotic mechanism.

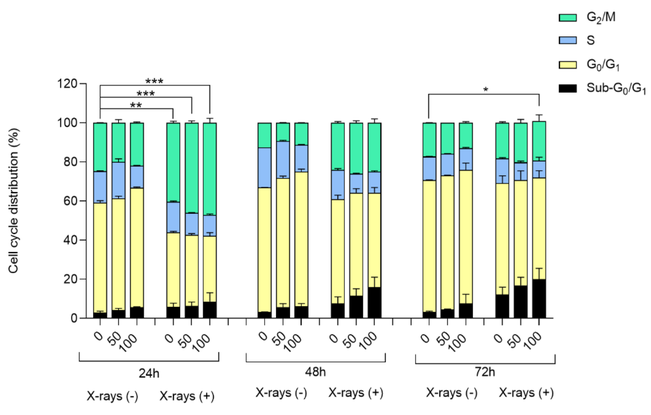

Figure 5: Cell cycle analysis. (a) Percentage distribution of HT-29 cells across the cell cycle phases (G0/G1, S, G2/M, and Sub-G0/G1) after treatment with 0, 50, or 100 µg/mL THPP@AuNPs@WS_2, with or without 2 Gy X-ray irradiation. Cell cycle analysis was performed at 24, 48, and 72 h post-irradiation. Results are shown as mean values ± S. D (n = 3), where ***p < 0.0002 and **p < 0.01 referring to G2/M bars and * p < 0.05 referring to Sub-G0/G1 bars. One-way analysis of variance (ANOVA) with Dunnett's post hoc tests was used for data comparison.

CONCLUSIONS

- 2D WS_2, AuNPs, and THPP derivative are engineered into a stable hybrid nanosystem.
- Biocompatibility and absence of proinflammatory responses are proven in PBMCs.
- NS-mediated radiosensitization is achieved under X-ray irradiation at 40 KeV, 2 Gy.
- The efficacy is validated in radioresistant human colorectal adenocarcinoma cells and Treatment promotes proliferation arrest and intra-cellular oxidative stress.

REFERENCES AND ACKNOWLEDGMENT

1. R. Zang et al. Journal of Material Chemistry B. 2024 (https://doi.org/10.1039/D4TB01787K). 2. G. Cenci et al. Materials Today Advances, 2026, (https://doi.org/10.1016/j.mtadv.2026.100956). 3. A.E. Del Rio Castillo et al. Materials Horizons 5, 2018 (https://doi.org/10.1039/C8MH00487K). 4. G. Bertoni et al. Scientific Reports, 6, 2016 (https://doi.org/10.1038/srep19168).

This work was supported by the European Union's Horizon Europe research and innovation programme under grant agreement no. 101099423 (PERSEUS)

PERSEUS

Find more information about PERSUS on our website!!!